TI Designs: TIDA-01587
10.8-V/30-W, >95% Efficiency, 4.3-cm^2, Power Stage Reference Design for Brushless DC Servo Drive

Description

This 15-W, 16-mm × 27-mm, power stage reference design drives and controls the position of the brushless DC (BLDC) motor operating from a three- to four-cell Li-ion battery. This highly-efficient solution is optimized with a very small form factor that easily fits into the motor and supports precise motor position control. The design is also capable of driving the motor at high speeds with position feedback. The reference design is protected for overcurrent and short circuit, and the onboard MCU provides UART connectivity, which enables controllability with any external controller.

Resources

TIDA-01587	Design Folder
DRV8304	Product Folder
CSD87502Q2	Product Folder
MSP430FR5949	Product Folder
TPS709	Product Folder
TVS3300	Product Folder

TI E2E™ Community — ASK Our E2E™ Experts

Features

- BLDC Servo Drive Operates at Voltage Ranging from 6-V to 16.8-V (Three- to Four-Cell Li-ion Battery)
- Supports 2.5-A_{RMS} Continuous, 5-A Peak Motor Winding Current
- Supports Trapezoidal and Sinusoidal Control for Permanent Magnet Motors
- Closed Loop 60° Electrical Position Control With Digital Hall Sensor Feedback for BLDC Motor
- Supports Position Control with Sinusoidal Excitation with Analog Hall Feedback
- Very Small PCB Form Factor of 16 mm × 27 mm
- Power Stage Efficiency > 95%, Without Heat Sink
- Increased Battery Life With High-Efficiency Power Stage, Low-Power MCU, and Low-Quiescent Current LDO
- Overcurrent, Shoot-Through, and Undervoltage Protection
- Provision for UART Wired Communication
- Operating Ambient Temperature: –20°C to +55°C

Applications

- Humanoids
- Vacuum Robots
- Robotic Lawn Mowers

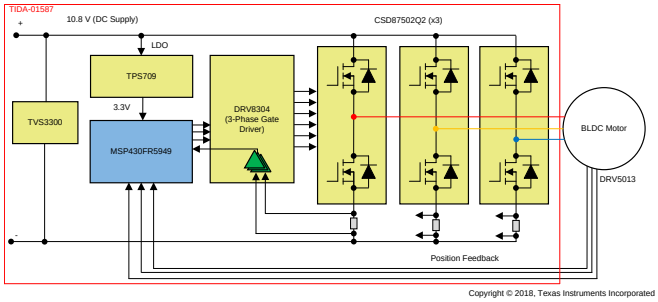

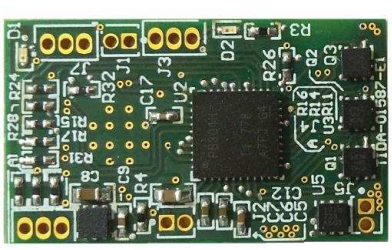

An IMPORTANT NOTICE at the end of this TI reference design addresses authorized use, intellectual property matters and other important disclaimers and information.

1 System Description

A humanoid robot is a type of service robot used in wide-end applications such as research applications where human access is risky, high-end toys used for teaching, dancing, and speaking, and more. Multiple motors are present in a typical humanoid depending upon the features and application requirement. The commonly used motors are brushed DC (BDC), brushless DC (BLDC), and sometimes stepper types. Figure 1 shows the examples of motor drive locations in a typical humanoid. The high-end or high-power motors are typically present in the neck, legs, shoulders, and so on. Low-end or low-power motors are used in other locations such as elbows, knees, fingers, and so on. The electronic drive used in these motors has the following requirements:

- Must be small enough to fit with the motor
- Must support accurate position and torque control
- Must have the sufficient holding torque capability

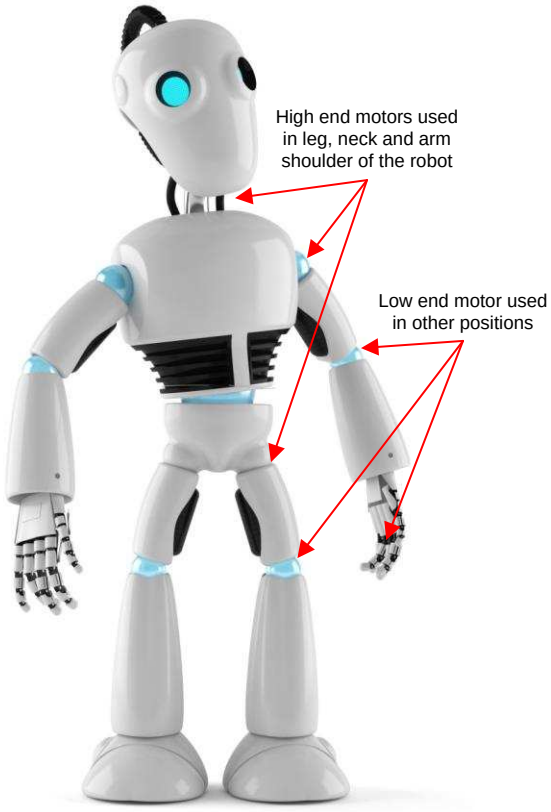

Figure 1. Typical Humanoid—Motor Drive Locations

Vacuum robots are another service robot widely used in consumer applications for cleaning. The motors used in vacuum robots have different requirements like high-speed rotation, high torque-slow speed operation, or position control depending on the functionality these motors support (for example, suction, wheel, side brush, position control of the robotic vision control motor, and so on). BDC, BLDC, or stepper motors are typically used. The electronic drives have similar requirements as said in the case of humanoids.

This three-phase BLDC power stage reference design can support the position control in a humanoid or the motor control in a vacuum robot. The design demonstrates the BLDC motor servo drive power stage in a very small form factor using the highly-integrated three-phase gate driver DRV8304 featuring a high level of integration and protection, reducing the overall BOM to a large extend.

The very small form factor and higher efficiency is also achieved by using the CSD87502Q2 offering two independent 30-V N-channel MOSFET in a SON 2×2 mm plastic package, having a low drain-to-source on-resistance ($R_{DS(on)}$) of 27 mΩ. The TPS709 LDO features a low-quiescent current (< 1 μA) and generates the low-noise, stable, 3.3-V power supply for the MCU. The MSP430FR5949 runs the position control algorithm by taking the position feedback signals from the motor, and offers trapezoidal and sinusoidal motor control. The TVS3300 provide surge voltage protection on input voltage supply.

The test report evaluates the board power capability, efficiency, overcurrent protection, peak current capability, and the position control with sufficient hold-up torque.

1.1 Key System Specifications

Table 1. Key System Specifications

PARAMETERS	SPECIFICATIONS
Input voltage	10.8-V DC (6-V minimum to 16.8-V maximum)
Rated output power	30 W
RMS winding current	2.5 A
Peak winding current	5 A
Inverter switching frequency	20 kHz (adjustable from 5 kHz to 100 kHz)
Feedback signals	DC bus voltage, analog or digital position feedback, low-side inverter leg currents
Protections	Overcurrent, input undervoltage, over temperature, shoot-through
Cooling	Natural cooling only, no heat sink
Operating ambient	–20°C to +55°C
Board specification	16 mm × 27 mm, 2-layer, 1-oz copper, 1.6-mm board thickness
Efficiency	> 95%

2 System Overview

2.1 Block Diagram

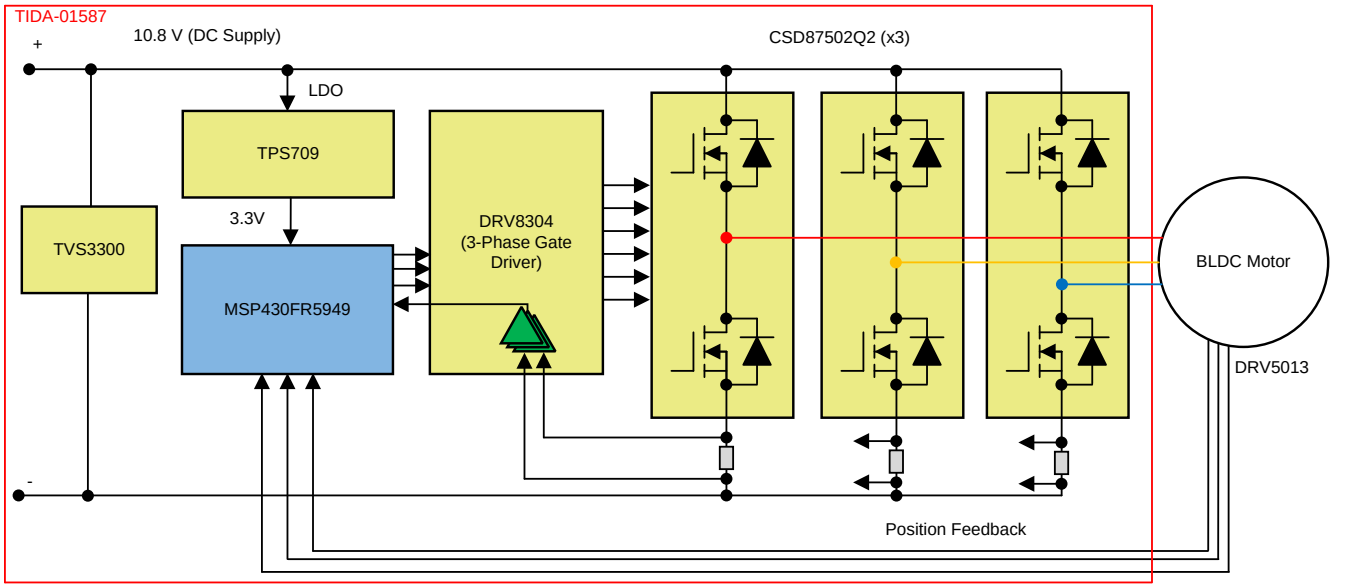

Figure 2. TIDA-01587 Block Diagram

2.2 Highlighted Products

2.2.1 DRV8304

The key requirements in selecting the gate driver are:

- Small form factor, three-phase gate driver with high level of integration and protection
- Support the operating voltage range with sufficient gate current
- Support the required minimum DC input voltage, still provides sufficient gate voltage for the external FET to operate at the minimum $R_{DS(on)}$
- Low power consumption

The reference design uses the three-phase gate driver DRV8304, which is specified for 6 V to 38 V, providing a maximum gate current of 150-mA source and 300-mA sink. The DRV8304 can support applications including field-oriented control (FOC), sinusoidal current control, and trapezoidal current control of BLDC motors. The DRV8304 device integrates three current-sense amplifiers (CSA) for sensing the phase currents of BLDC motors for optimum FOC and current-control system implementation. An AUTOCAL feature automatically calibrates the CSA offset error for accurate current sensing.

The DRV8304 device is based on smart gate-drive (SGD) architecture to eliminate the need of any external gate components (resistors and Zener diodes) while fully protecting the external FETs. The SGD architecture optimizes dead time to avoid any shoot-through conditions, provides flexibility in reducing electromagnetic interference (EMI) by gate slew-rate control and protects against any gate-short conditions. Strong pulldown current also prevent any dv/dt gate turnon. The gate driver provide overcurrent and short-circuit protection by MOSFET V_{DS} monitoring.

2.2.2 CSD87502Q2

The key requirements in selecting the power stage MOSFETs are:

- Low $R_{DS(on)}$ and gate charge for high efficiency operation
- Small form factor
- Low thermal resistance and provision for heat dissipation to PCB

The reference design uses the CSD87502Q2, which is a 30-V, 27-mΩ N-channel device with dual independent MOSFETs in a SON 2×2-mm plastic package. The dual FETs feature a low $R_{DS(on)}$ that minimizes losses and offers low component count for space-constrained applications. The low junction-to-ambient thermal resistance with the help of thermal pads on the package allows easy heat dissipation.

2.2.3 MSP430FR5949

The MSP430™ ultra-low-power (ULP) FRAM platform combines uniquely embedded FRAM and a holistic ultra-low-power system architecture, allowing innovators to increase performance at lowered energy budgets. FRAM technology combines the speed, flexibility, and endurance of SRAM with the stability and reliability of flash at much lower power.

The MSP430 ULP FRAM portfolio consists of a diverse set of devices featuring FRAM, the ULP 16-bit MSP430 CPU, and intelligent peripherals targeted for various applications. The ULP architecture showcases seven low-power modes, optimized to achieve extended battery life in energy-challenged applications.

The device has a 16-bit RISC architecture supporting up to a 16-MHz clock. The device has five 16-bit timers with up to seven capture/compare registers each. The seven capture/compare registers helps to realize six PWM signals for three-phase sine control with a single time base. The device has 32-bit hardware multiplier and a 12-bit analog-to-digital converter (ADC) with internal reference and sample-and-hold and up to 16 external input channels. The enhanced serial communication allows easy communication with master controller in different service robots.

2.2.4 TPS709

The TPS70933 linear regulator is an ultra-low, quiescent current device designed for power-sensitive applications. The LDO can work up to a 30-V input voltage, which makes it ideal for up to six-cell Li-ion battery supply application. A precision band-gap and error amplifier provides 2% accuracy over temperature. A quiescent current of only 1 μA makes this LDO ideal for battery-powered, always-on systems that require very little idle-state power dissipation. This device has thermal-shutdown, current limit, and reverse-current protections for added safety. The TPS70933 linear regulator is available in WSON-6 and SOT-23-5 packages.

2.2.5 TVS3300

The TVS3300 is a transient voltage suppressor that provides robust protection for electronic circuits exposed to high transient voltage events. Unlike a traditional TVS diode, the TVS3300 precision clamp triggers at a lower breakdown voltage and regulates to maintain a flat clamping voltage throughout a transient overvoltage event. The lower clamping voltage combined with a low dynamic resistance enables a unique TVS protection solution that can lower the voltage a system is exposed during a surge event by up to 30% in unidirectional configuration and up to 20% in bidirectional configuration when compared to traditional TVS diodes.

The TVS3300 is a unidirectional precision surge protection clamp with a 33-V working voltage designed specifically to protect systems with mid-voltage rails in industrial, communication, and factory automation applications. The TVS3300 has a fast response time when surge current is applied so there is no overshoot voltage during clamping, making it ideal to replace traditional TVS and Zener diodes.

The TVS3300 is available in two small footprint packages which, when used in place of an industry standard SMB package, can reduce footprint by 94% (WCSP package) and 79% (SON package) for space constrained applications. Both package options robustly dissipate the surge power and provide up to 58% lower leakage current compared to traditional TVS diodes in SMA and SMB package.

2.3 System Design Theory

2.3.1 DC Voltage Input to the Board

The board gets the DC input voltage through the jumper J5 as shown in Figure 3. The TVS3300 is a surge protection clamp provided at the input to protect the circuit from input voltage surges. The design is optimized for a three-cell Li-ion battery and can support up to four-cell applications, having a maximum voltage of 16.8 V.

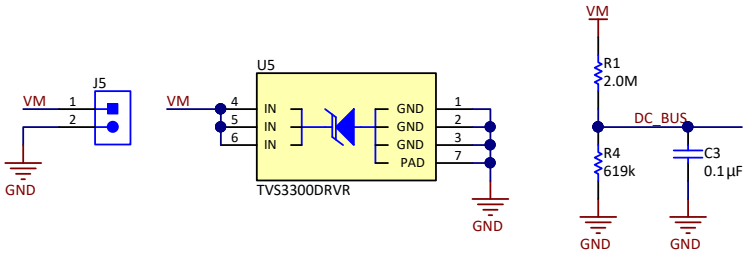

Figure 3. Schematic of Battery Power Input Section

The input supply voltage PVDD is scaled using the resistive divider network, which consists of R1, R4, and C3, and fed to the MCU. Considering the maximum voltage for the MCU ADC input as 3.3 V, the maximum DC input voltage measurable by the MCU is calculated as in Equation 1.

$$V_{DC}^{max} = V_{ADC\_DC}^{max} \times \frac{(619\ k\Omega + 2000\ k\Omega)}{619\ k\Omega} = 3.3 \times \frac{(619\ k\Omega + 2000\ k\Omega)}{619\ k\Omega} = 13.96\ V \quad (1)$$

Considering a 10% headroom for this value, the maximum recommended voltage input to the system is 13.96 × 0.9 = 12.56 V. So for a power stage operating from three-cell Li-ion, having a maximum operating voltage of 12.6 V, this voltage feedback resistor divider is ideal. Also, this choice gives optimal ADC resolution for a system operating from 6 V to 12.6 V.

2.3.2 Power Stage Design: Three-Phase Inverter

The three-phase inverter is realized using three dual MOSFET blocks CSD87502Q2, as shown in Figure 4. Each CSD87502Q2 block consists of two independent 30-V, 27-mΩ N-channel MOSFETs in a SON 2×2-mm plastic package.

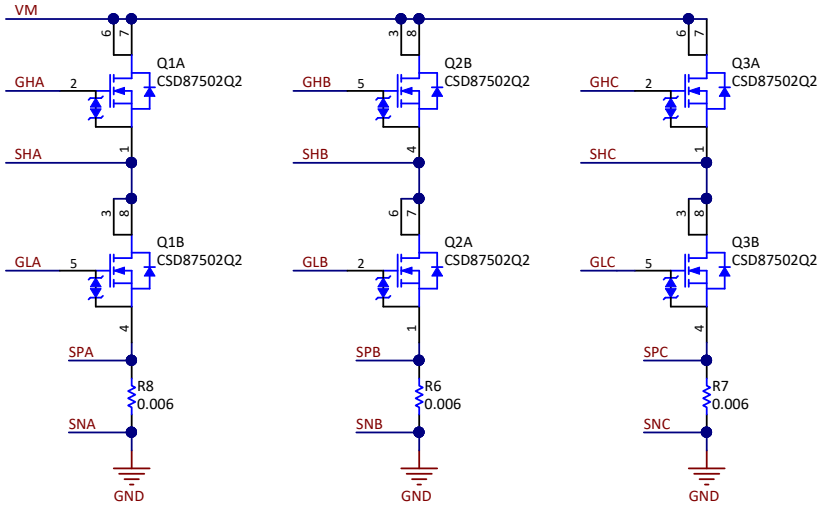

Figure 4. Schematic of Three-Phase Inverter

The resistors R6, R7, and R8 are used for inverter leg current sensing. The voltage across the sense resistor is fed to the MCU through the current shunt amplifiers in the DRV8304.

2.3.3 Selecting the Sense Resistor

The selection of sense resistor depends on different factors as follows:

- Power dissipation in the sense resistor
- Offset error voltage and gain of the current sense amplifier
- Peak current to be sensed

The sense resistors are designed to carry a continuous nominal RMS current of 2.5 A and a peak current of 5 A. A high sense resistance value increases the power loss in the resistors. A low sense resistor value increases the error due to input offset voltage of the current sense amplifier at high gain. If the current-sense amplifier is used without offset calibration, select the sense resistor value such that the sense voltage across the resistor is sufficiently higher than the op-amp input offset voltage to reduce the effect of the offset error. The TLV9061 has a maximum input offset error voltage of 1.5 mV. The reference design uses a 0.006-Ω sense resistor, and the power loss in sense resistor can be calculated using Equation 2:

$$\text{Power loss in the resistor} = I_{RMS}^2 \times R_{SENSE} = 2.5^2 \times 0.006 = 0.0375 \text{ W} \quad (2)$$

At a 5-A peak current, using Equation 2, the power loss in the resistor = 0.15 W.

2.3.4 Power Stage Design: Three-Phase Gate Driver

Figure 5 shows the schematic of the DRV8304 gate driver. C17 is the DVDD decoupling capacitor that must be placed close to DRV8304. C6 and C7 are the charge pump capacitors. These capacitors are selected to provide a stable charge pump voltage with minimum ripple. VM is the DC supply input; in this case, it is the battery voltage of 10.8 V. C1 and C4 are the bulk ceramic capacitor placed near the inverter bridge.

The gate drive circuit is designed, and the different resistors are selected to meet the specification as per Table 2.

Table 2. Design Specification of DRV8304 Gate Driver

PARAMETER	DEFAULT VALUE	CIRCUIT DESCRIPTION
MODE (PWM mode)	6× PWM control mode	MODE pin tied to AGND
I_{DRIVE} (gate source and sink current)	15-mA source, 30-mA sink	IDRIVE pin tied to AGND
V_{DS} (monitor reference voltage)	0.15 V	VDS pin tied to AGND
GAIN (current sense amplifier gain)	40 V/V	GAIN pin tied to 3.3 V (DVDD)
V_{REF}	3.3 V	Support bidirectional current sensing
CAL	Controllable through MCU	Amplifier calibration through MCU

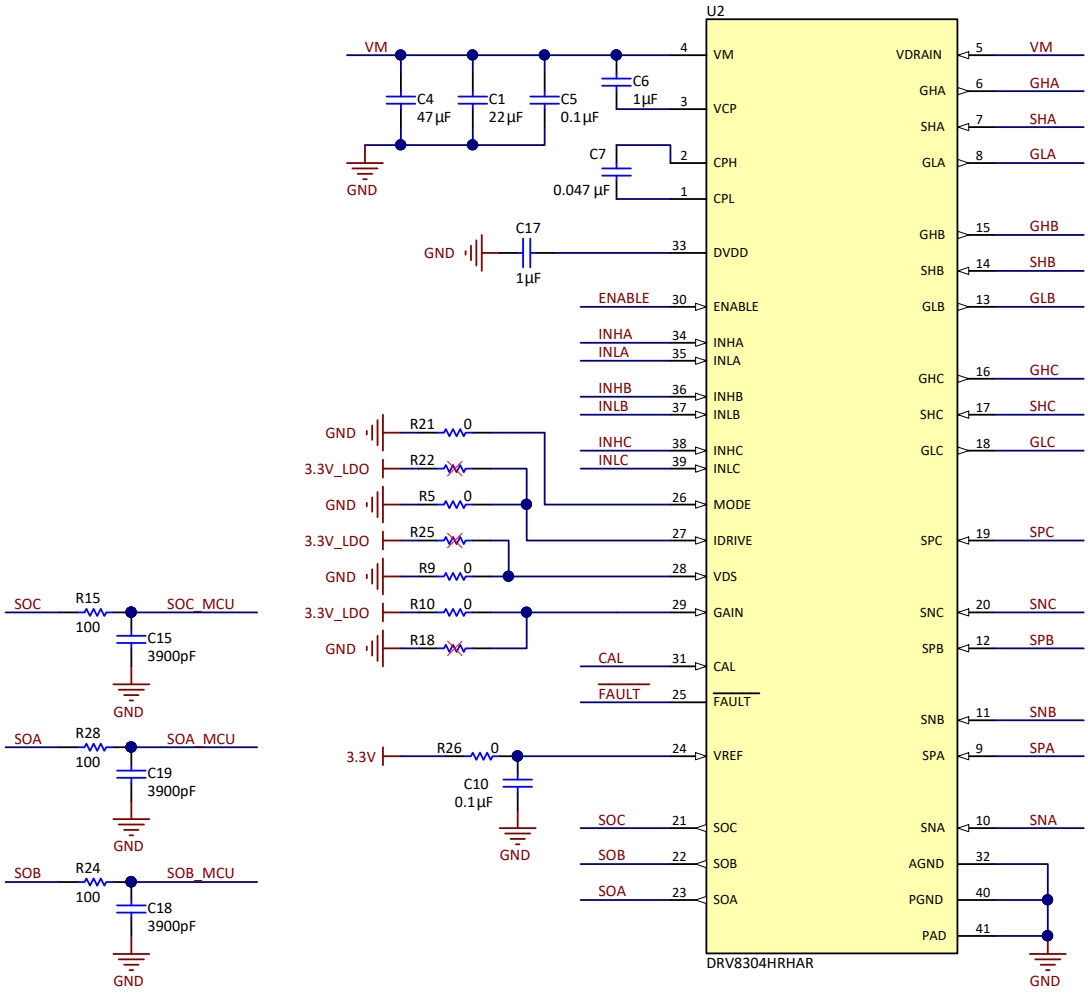

Figure 5. Schematic of DRV8304 Gate Driver

2.3.5 Current Sense Amplifier

The SOx pin on the DRV8304 outputs an analog voltage equal to the voltage seen across the SPx and SNx pin multiplied by the gain setting (CSA_GAIN). The gain setting is adjustable between four different levels (5, 10, 20, and 40 V/V). The amplifier as shown in Figure 6 can be used to monitor the current through the half-bridges and the current is approximately calculated using Equation 3.

$$I_{SENSE} = \frac{\frac{V_{REF}}{2} - SO_X}{CSA\_GAIN \times R_{SENSE}} \quad (3)$$

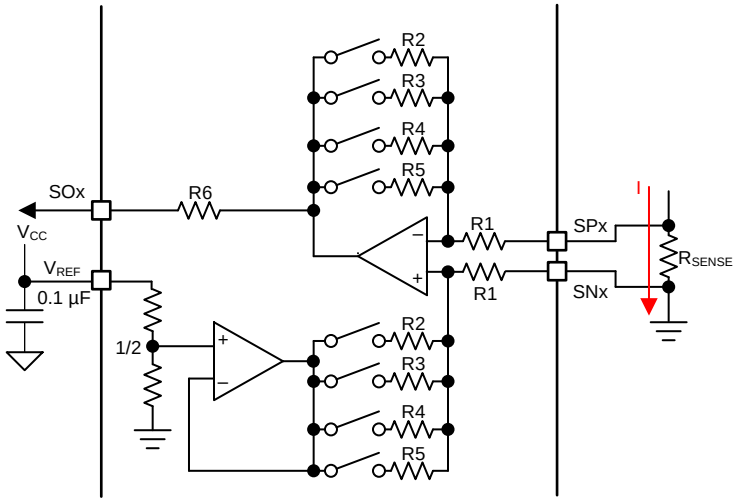

Figure 6. DRV8304 Current Sense Amplifier

The sense amplifier gains on the DRV8304 and sense resistor value are selected based on the target current range, V_{REF}, sense resistor power rating, and temperature. In bidirectional operation of the sense amplifier, the dynamic range at the output is approximately:

$$V_O = (V_{REF} - 0.25\ V) - \frac{V_{REF}}{2}$$

where

- V_{REF} = 3.3 V (4)

The required current sense range for the reference design is from –5 A to +5 A. The DRV8304 has an SOx output linear range of 0.25 V to V_{REF} – 0.25 V (from the V_{LINEAR} specification). The differential range of the sense amplifier input is –0.3 V to +0.3 V ($V_{SP,DIF}$).

$$R_{SENSE} = \frac{1.4\ V}{A_V \times I_{SENSE}} \quad (5)$$

$$V_O = (3.3\ V - 0.25\ V) - \left(\frac{3.3\ V}{2}\right) = 1.4\ V$$

With R_{SENSE} = 0.006 Ω and an amplifier gain of 40 V/V, using Equation 5, the design allows a current sensing from –5.8 A to +5.8 A, which means 15% over rated from the required rated peak current of 5 A.

2.3.6 MSP430FR5949 MCU

Figure 7 shows the configuration of MSP430FR5949 MCU. The reference design uses 4.7-µF decoupling capacitors (C2, C12) at AVCC and DVCC pins. A 0.1-µF capacitor has been added to obtain the best performance at a high frequency. The Timer B module of the MCU is used for PWM generation. The seven capture/compare registers helps to realize six PWM signals for three-phase sine control, with a single time base. The six PWM signals are generated at TB0.1 to TB0.6 pins. The digital Hall signals are connected to port 1 of the MCU. For an analog position signal interface, configure the pins as analog pins. The MCU is configured for sensing different analog signals like the inverter leg currents, DC bus voltage, position reference signals, and so on. The provision for UART communication is also provided.

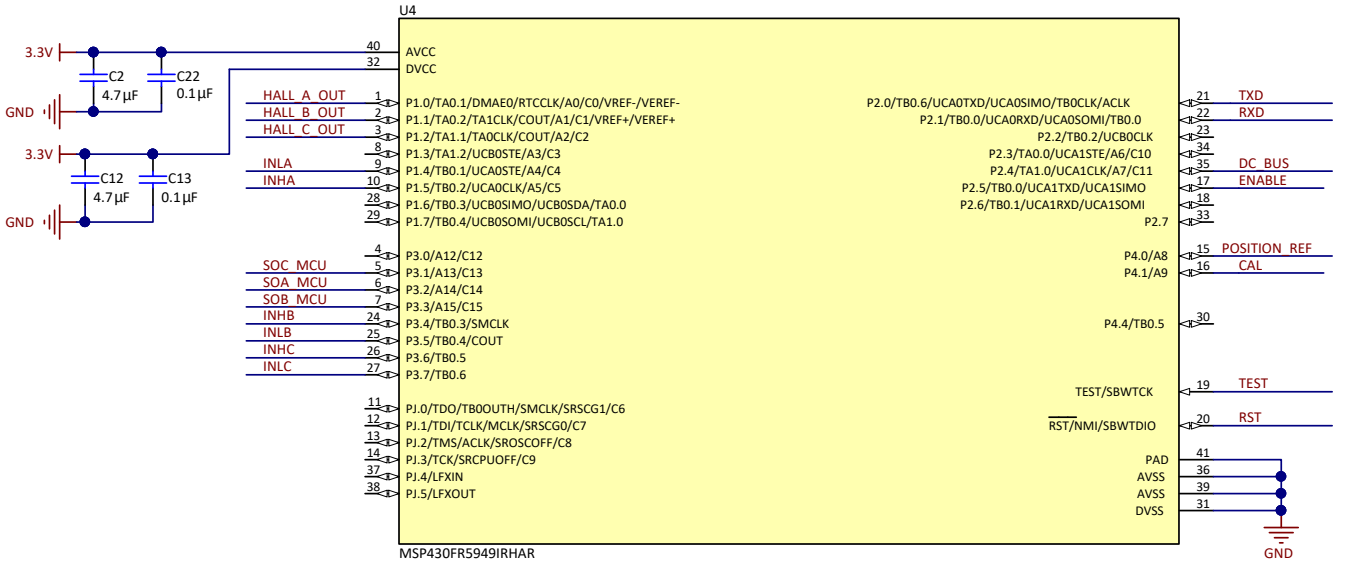

Figure 7. Schematic of MSP430FR5949

2.3.7 Motor Position Feedback

Figure 8 shows the position feedback interface from the motor to the reference design board. By default, the reference design is configured to sense digital Hall sensor output, which is connected to port 1 of MCU. The reference design can support analog position feedback also; in that case, connect the sensor output to same port pins and configure the pins as an analog input pin of the MCU ADC.

The position reference signal can be connected to J7 by connecting an external potentiometer (POT).

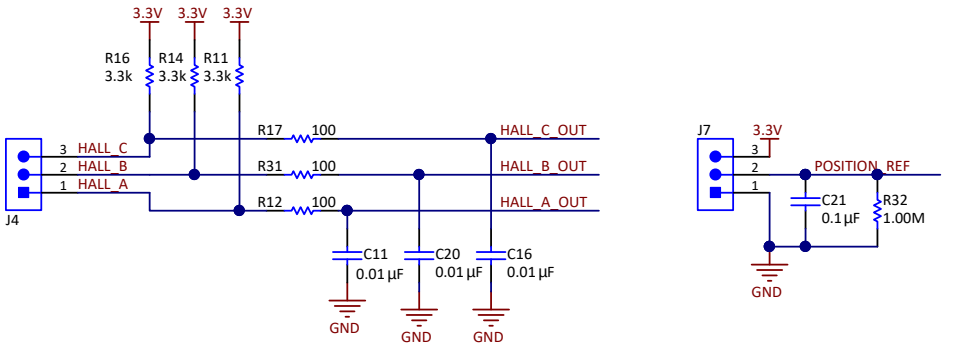

Figure 8. Schematic of Position Feedback

2.3.8 LDO

The reference design uses the ultra-low quiescent current, LDO linear regulator TPS70933 to generate the 3.3-V power supply for the MCU from the input voltage of 10.8 V. Figure 9 shows the schematic of the LDO circuit.

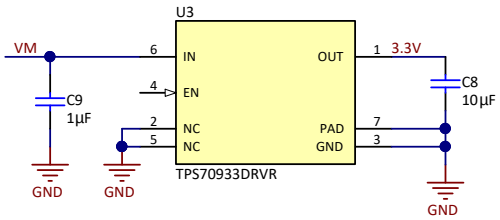

Figure 9. Schematic of 3.3-V LDO

The selection of LDO depends on the wide input voltage support (in this design, from 6 V to 16.8 V), the load current, and power dissipation. Power dissipation depends on input voltage and load conditions. Power dissipation (P_{DISS}) is equal to the product of the output current and the voltage drop across the output pass element, as given in Equation 6.

$$P_{DISS} = (V_{IN} - V_{OUT}) \times I_{OUT} \quad (6)$$

Assuming a nominal LDO load current of 20 mA, the power dissipation at V_{IN} = 16.8 V can be calculated as:

P_{DISS} = (16.8 – 3.3) × 0.02 = 0.27 W

Table 3 shows the specifications of the LDOs used in this reference design. At lower input voltage, the power dissipation in the LDO reduces. This reference design assumes a maximum LDO output current of 30 mA when operating from a three-cell Li-ion battery.

Table 3. Specification of Buck Converter

PARAMETER	DESIGN SPECIFICATION
Input voltage	6 V to 16.8 V (10.8-V nominal)
Output voltage	3.3 V
Maximum output current	30 mA (at 10.8-V input voltage)

3 Hardware, Software, Testing Requirements, and Test Results

3.1 Required Hardware and Software

3.1.1 Hardware

3.1.1.1 Connector Configuration of TIDA-01587

Figure 10 shows the connector configuration of this reference design, which features:

- Two-terminal input for power supply (J5): This pin is used to connect the input DC supply from the battery. The positive and negative terminals can be identified as shown in Figure 10.
- Three-terminal output for motor winding connection: The phase output connections for connecting to the BLDC motor winding marked as Phase A, Phase B, and Phase C as shown in Figure 10.
- Three-pin connector J3: This connector is used for external UART communication interface. The RX and TX pins enable the communication with external master controller. The FAULT pin of this connector gives indication on FAULT signal from gate driver DRV8304.
- Two-pin connector J1: This is the programming connector for the MSP430FR5949 MCU, along with the 3.3-V lines at connector J2. The two-wire Spy-Bi-Wire protocol is used to program the MSP430FR5949. See the MSP430FR5949 development tools for programming options with an external JTAG interface.
- Three-pin connector J7: This connector interfaces the position reference from external potentiometer. A 20k POT can be used.
- Three-pin connector J4: This connector interfaces hall senor position signal from the motor.

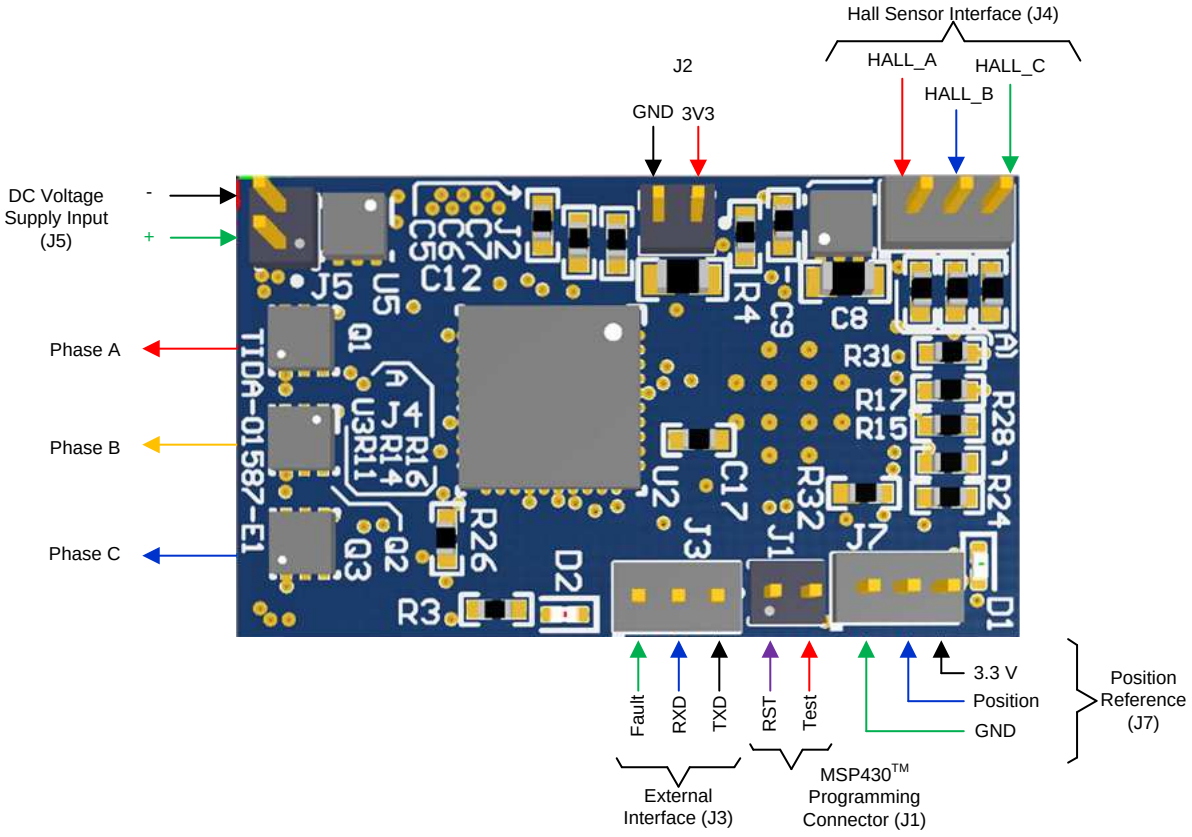

Figure 10. PCB Connectors

3.1.1.2 Procedure for Board Bring-up and Testing

Follow this procedure for board bring-up and testing:

1. Remove the motor connections from the board and power on the input DC supply. Make sure that a minimum of a 8-V DC input is applied and the 3.3 V is generated in the board.
2. Program the MCU. Make sure that the configuration in the program is done as per Section 3.1.2.
3. Remove the programmer, and switch off the DC input supply.
4. Connect the phase outputs from the board to the motor winding terminals.
5. Use a DC power supply with current limit protection and apply 8-V DC to the board. The motor starts rotating and stops at the position mentioned by the position reference.
6. To change direction, switch off the DC input, and correct the logic in the program and re-load the same in to the MCU.

3.1.2 Software

3.1.2.1 High-Level Description of Application Firmware

The reference design firmware offers the following features and user controllable parameters:

- 60° electrical position control using digital hall sensor position feedback
- BLDC motor speed control using trapezoidal control

Table 4 lists the firmware system components.

Table 4. TIDA-01587 Firmware System Components

SYSTEM COMPONENT	DESCRIPTION
Development and emulation	Code Composer Studio™ (CCS) version 7
Target controller	MSP430FR5949
PWM frequency	20-kHz PWM (default), programmable for higher and lower frequencies
Interrupts	Port 1 Interrupts enabled on P1.0, P1.1, and P1.2 corresponds to digital hall sensor interface
PWM generation—Timer configuration	PWMs: TB0.1–TB0.6 ; CLOCK = 16 MHz, PWM frequency set for 20 kHz
Position feedback—Hall sensor signals	P1.0 → HALL A P1.1 → HALL B P1.2 → HALL C
ADC channel assignment	A7 → DC bus voltage feedback A8 → Position reference from potentiometer A13 → Phase C inverter leg current A14 → Phase A inverter leg current A15 → Phase B inverter leg current
MCU digital inputs/output and communication	P2.5 → ENABLE signal for DRV8304 P2.0 → UART TXD P2.1 → UART RXD P4.1 → CAL pin of DRV8304

3.1.2.2 Customizing the Reference Code

Select the main.c file. Parameters exist at the top of the file that can be optimized and are included as the configuration variables. The following section of code shows these parameters:

```
#define PWM_PERIOD 400 // PWM Frequency (Hz) = 16MHz / ((2*PWM_PERIOD) - 1)
#define DUTY_CYCLE 70 // Input Duty Cycle inversely relative to PWM_PERIOD
#define POLES 8     // Number of poles in motor
#define Gear_Ratio 1  // Gear ratio in the Motor
```

3.1.2.2.1 PWM_PERIOD

The PWM_PERIOD parameter sets the value in capture and compare register 0 of Timer_B0. The Timer_B0 is initialized to operate at a 16-MHz clock. Use Equation 7 to calculate the PWM frequency. The TIMER_A0 PWM is configured in up-down mode.

$$\text{PWM Frequency}\,(\text{Hz}) = \frac{16\ \text{MHz}}{\left((2 \times \text{PWM\_PERIOD}) - 1\right)} \tag{7}$$

For example, with PWM_PERIOD = 400, PWM frequency ≈ 20 kHz.

3.1.2.2.2 DUTY_CYCLE

Adjust this parameter to control the speed of the motor. This parameter is inversely related to PWM_PERIOD.

3.1.2.2.3 POLES

This parameter is the number of magnetic poles in the rotor of motor. The algorithm sets the 60° electrical position control using BLDC trapezoidal control, which means the resolution accuracy is 60° electrical.

The equivalent mechanical position resolution accuracy can be calculated from the number of magnetic poles in the rotor (p).

$$\text{Mechanical Angle}\,(\theta_m) = \frac{\text{Electrical Angle}\,(\theta_e)}{\left(\frac{p}{2}\right)} \tag{8}$$

For example, with p = 8, Mechanical resolution angle from motor = 15°. If the motor has a gear with 10:1 gear ratio, then:

$$\text{Equivalent mechanical position resolution} = \frac{\text{Mechanical resolution angle from motor}}{\text{Gear ratio}} = 1.5°$$

3.2 Testing and Results

3.2.1 Test Setup

The test is performed with a BLDC motor at 10.8-V DC with trapezoidal and sinusoidal control. Figure 11 shows the test setup.

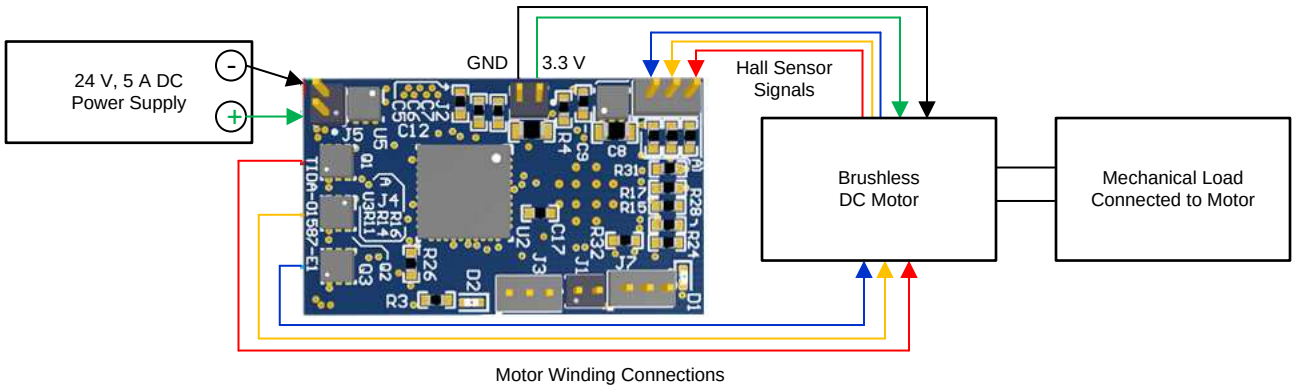

Figure 11. Load Test Setup

3.2.2 Test Results

3.2.2.1 3.3-V Power Supply Generated by the LDO

Figure 12 shows the 3.3 V generated from the LDO. The ripple in the 3.3-V rail is less than 15 mV.

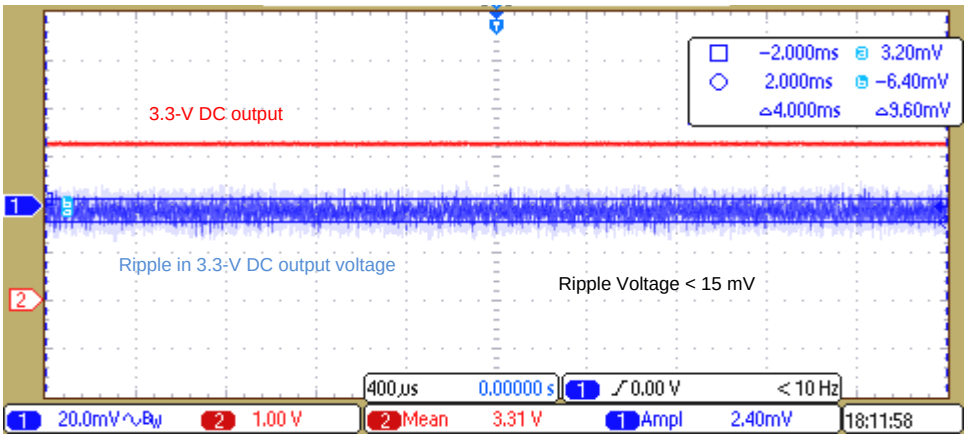

Figure 12. 3.3 V Generated by TPS70933

3.2.2.2 DRV8304 Gate Driver Output Voltage

Figure 13 shows the high-side and low-side gate drive output voltage of DRV8304 at a DC bus voltage of 10.8-V DC. The gate drive voltage is approximately 9.5 V, which means effective gate driving of standard MOSFETs. Figure 14 shows the gate drive voltage of the DRV8304 at a lower DC bus voltage of 6 V. The gate drive output voltage is approximately 4.5 V. Figure 15 shows the gate drive voltage of the DRV8304 at a higher DC bus voltage of 17 V. The gate drive output voltage is approximately 9.5 V.

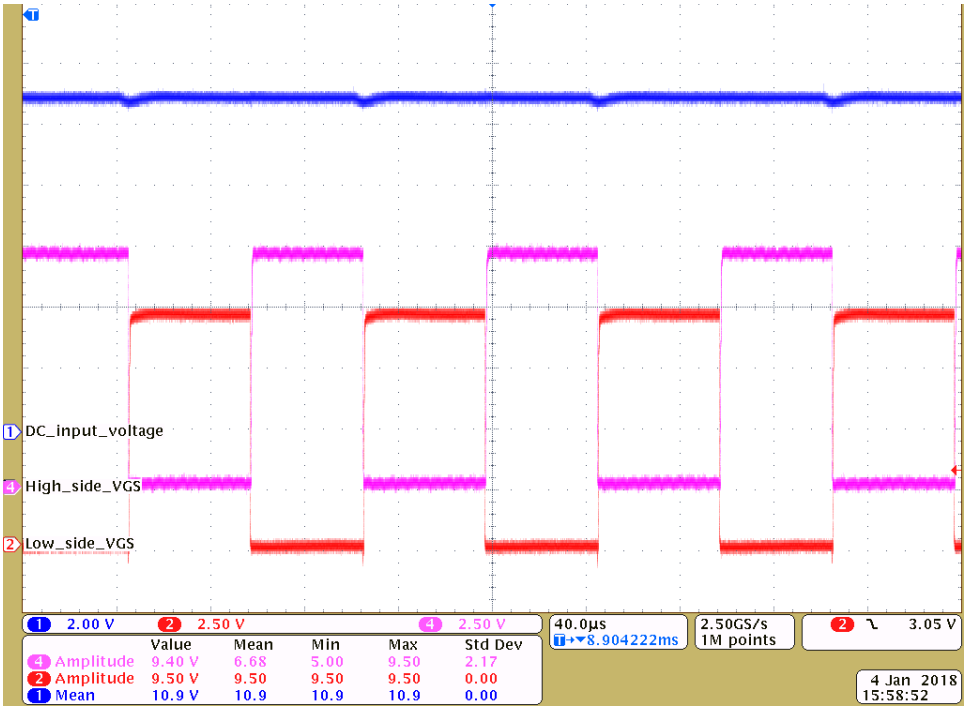

Figure 13. Low-Side and High-Side Gate Drive Voltage at 10.8-V DC

Figure 14. Low-Side and High-Side Gate Drive Voltage at 6-V DC

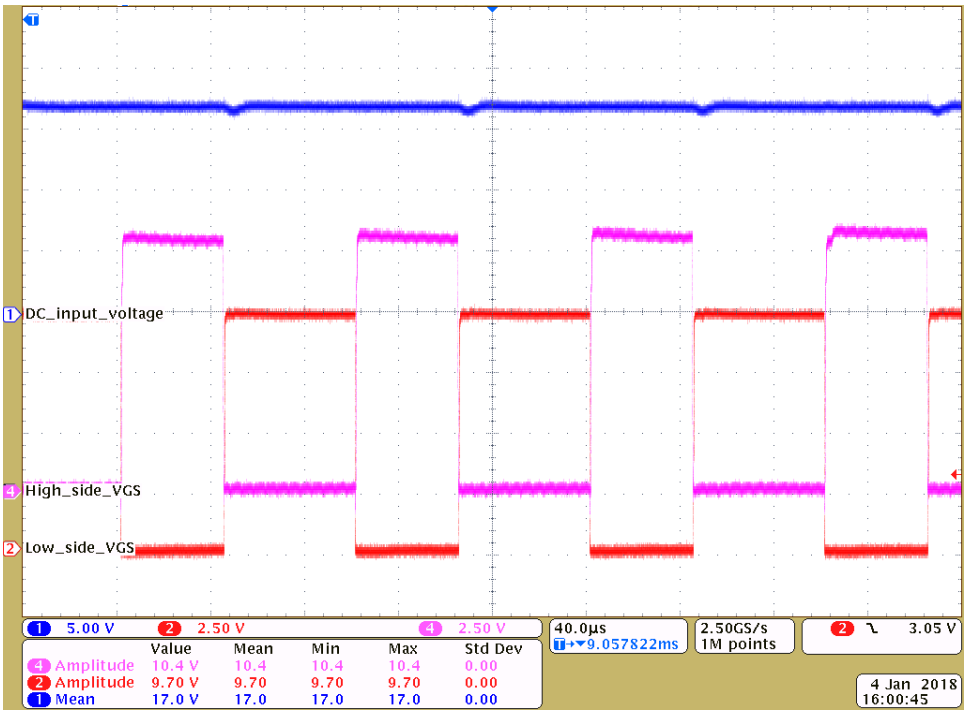

Figure 15. Low-Side and High-Side Gate Drive Voltage at 17-V DC

3.2.2.3 Dead Time From DRV8304

The dead time (t_{DEAD}) is measured as the time between turning off one of the half bridge MOSFETs and turning on the other. The hardware version of DRV8304 inserts a fixed dead time of 120 ns. Figure 16 and Figure 17 shows the high-side and low-side gate source voltage from the DRV8304, which shows the dead time inserted by the DRV8304 at both the edges of the PWM.

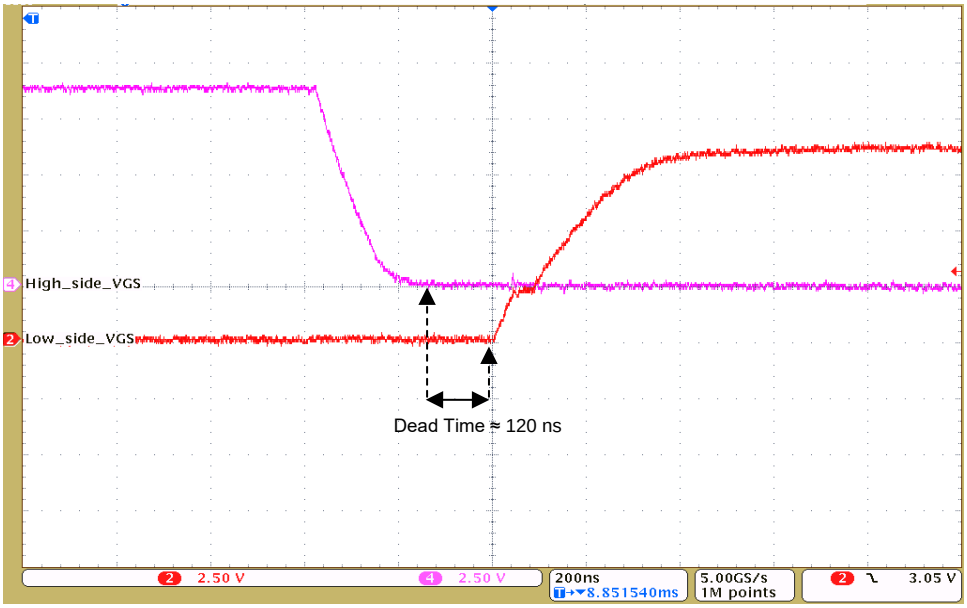

Figure 16. Dead Time at Rising Edge of Low-Side V_{GS}

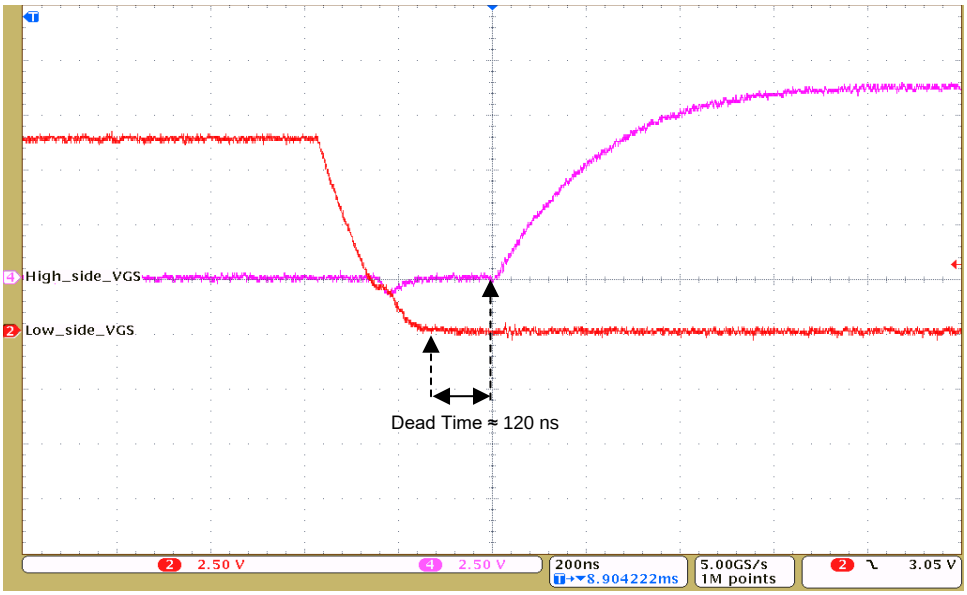

Figure 17. Dead Time at Trailing Edge of Low-Side V_{GS}

3.2.2.4 MOSFET Switching Waveforms

Figure 18 to Figure 21 show the V_{DS} and V_{GS} waveforms of the low-side and high-side MOSFETs at a gate current of the DRV8304 (I_{DRIVE}) is set at a 15-mA source (the low gate charge of the CSD87502Q2 allows low source current) and a 30-mA sink current. Switching waveforms are clean without much overvoltage ringing due to the following:

- Small size CSD87502Q2 with two FETs in same package allows reduced PCB parasitic and hence reduces the phase node voltage ringing.
- The current controlled gate driver with slew rate control helps to optimize the switching.
- The I_{DRIVE} and T_{DRIVE} features of the gate driver helps to shape the gate current to optimize the switching.

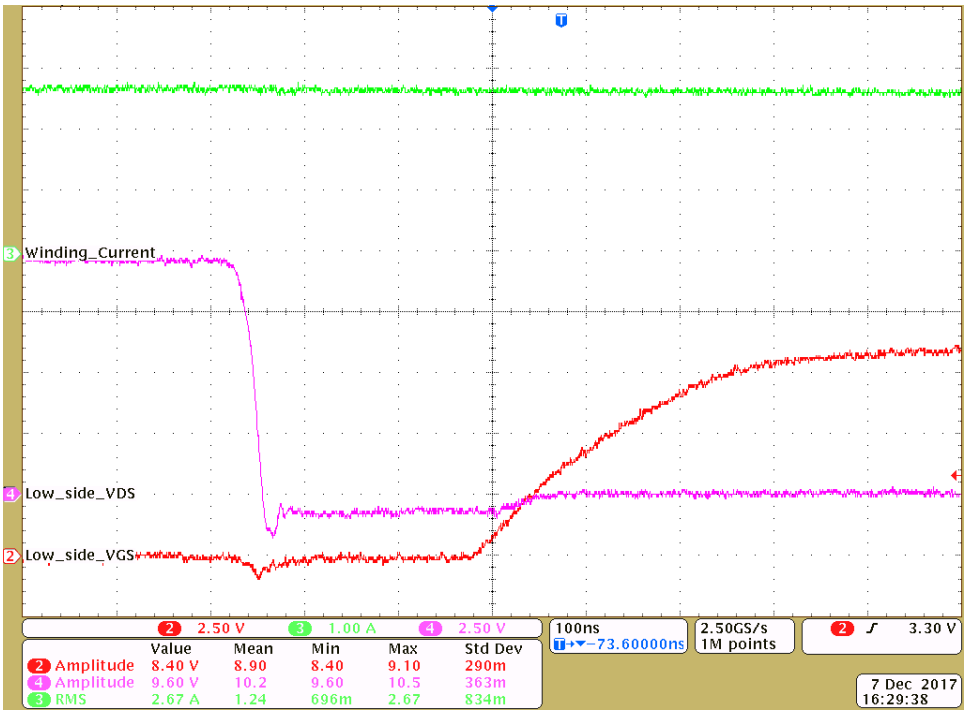

Figure 18. Low-Side FET Turnon: Low-Side V_{GS} and V_{DS} at 2-A Winding Current

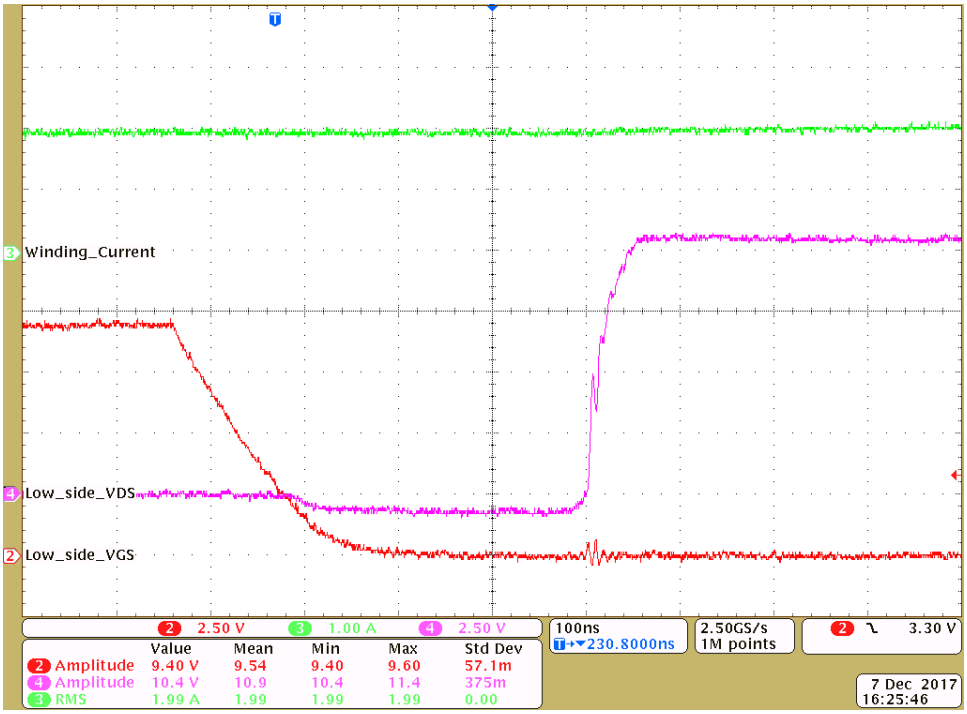

Figure 19. Low-Side FET Turnoff: Low-Side V_{GS} and V_{DS} at 2-A Winding Current

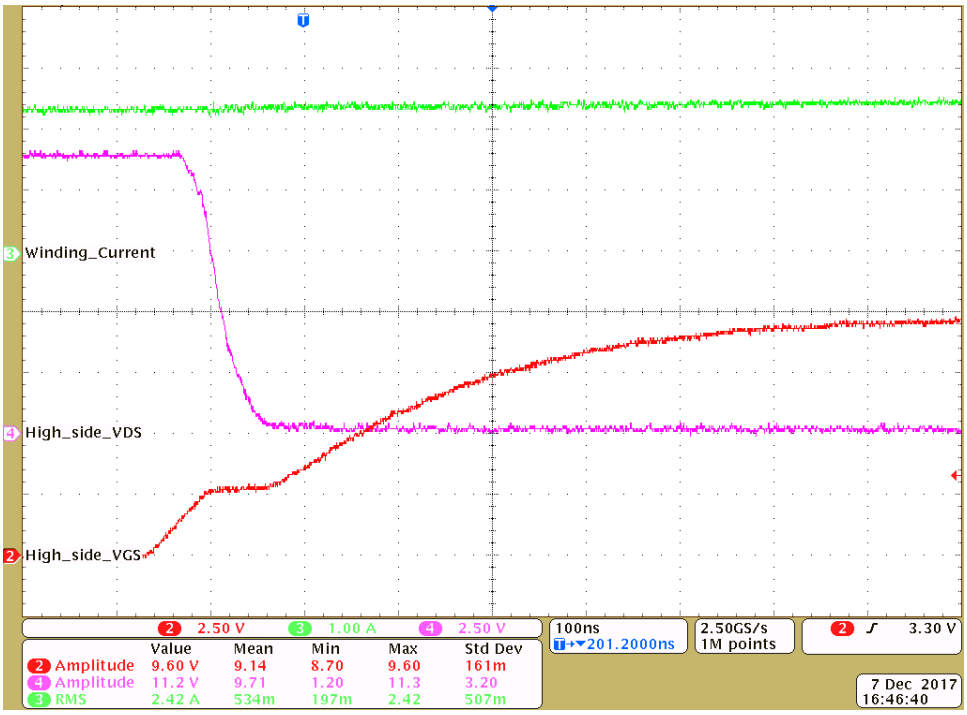

Figure 20. High-Side FET Turnon: High-Side V_{GS} and V_{DS} at 2-A Winding Current

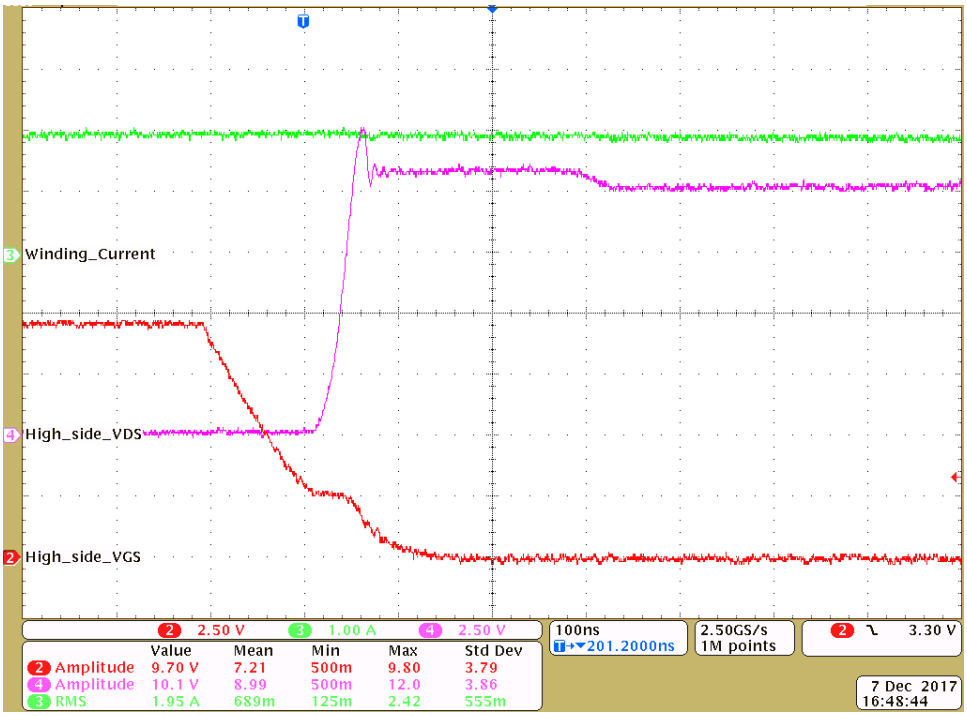

Figure 21. High-Side FET Turnoff: High-Side V_{GS} and V_{DS} at 2-A Winding Current

3.2.2.5 Load Test

The load test is done with test setup as shown in Figure 11. Table 5 lists the load test results. Figure 22 shows the test results with trapezoidal control at 2.28-A_{RMS} winding current and 100% duty cycle, and Figure 23 shows the results thermal image of the board after 10 minutes of continuous running. The maximum temperature observed on the MOSFET is 81.4°C. Figure 24 shows the test results with sinusoidal control at a 2.37-A_{RMS} winding current, and Figure 25 shows the thermal image of the board after 10 minutes of continuous running. The maximum temperature observed on the MOSFET is 85.9°C.

Figure 24 shows the test results with sinusoidal control at 2.5-A winding current.

Table 5. Load Test Results at 10.8-V DC

CONTROL METHOD	VDC (V)	IDC (A)	WINDING CURRENT (RMS) (A)	INPUT POWER (W)	MAXIMUM IC TEMPERATURE (°C)
Trapezoidal control	10.8	2.70	2.28	29.16	81.4
Sinusoidal control	10.8	2.72	2.37	29.4	85.9

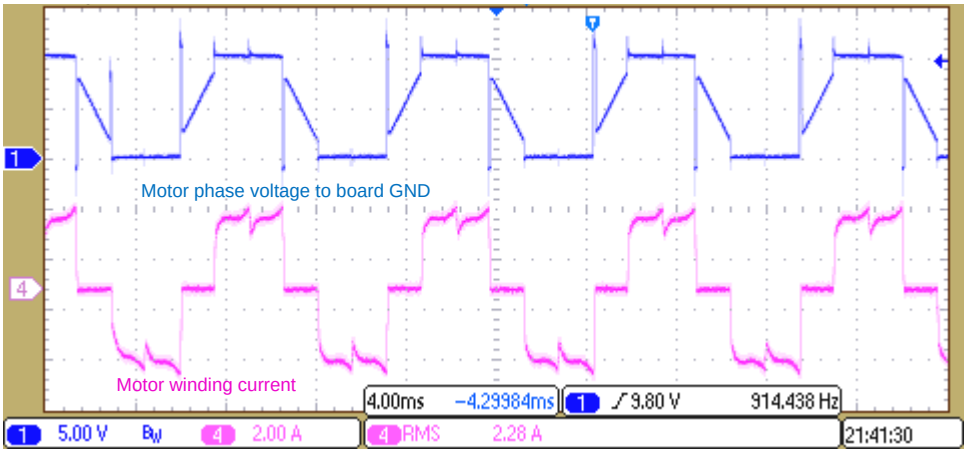

Figure 22. Load Test Results With Trapezoidal Control at 2.28-A_{RMS} Winding Current, 100% Duty Cycle

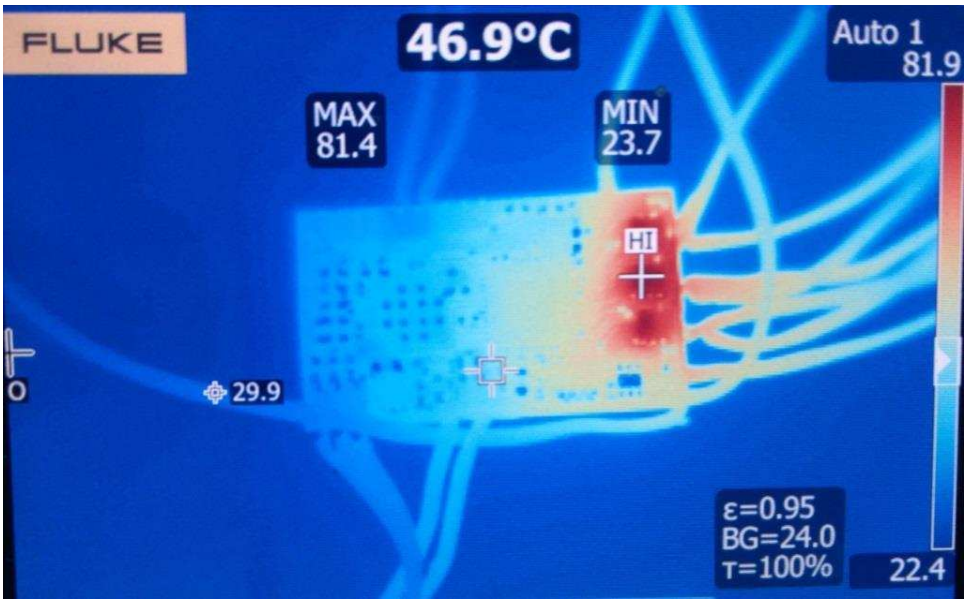

Figure 23. Thermal Image of Board With Trapezoidal Control at 2.28-A_{RMS} Winding Current, 100% Duty Cycle

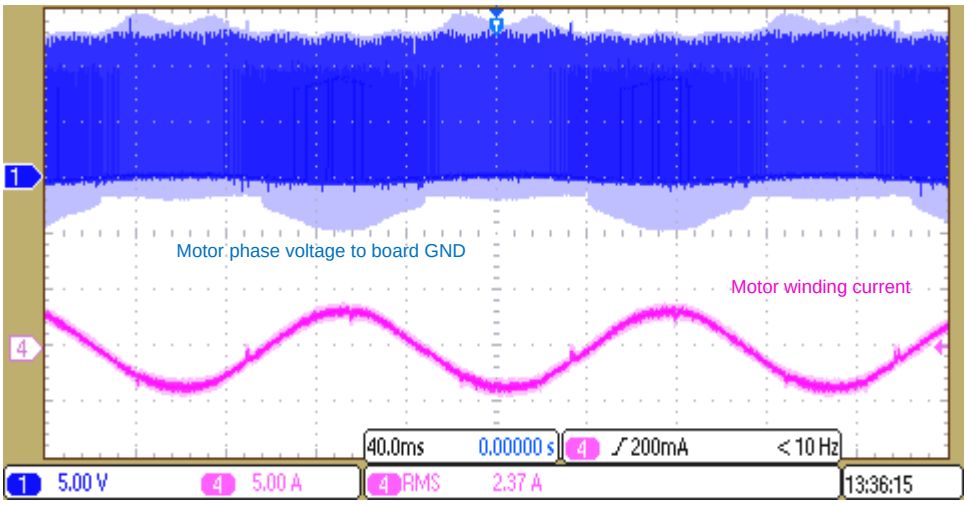

Figure 24. Load Test Results With Sinusoidal Control at 2.37-A_{RMS} Winding Current

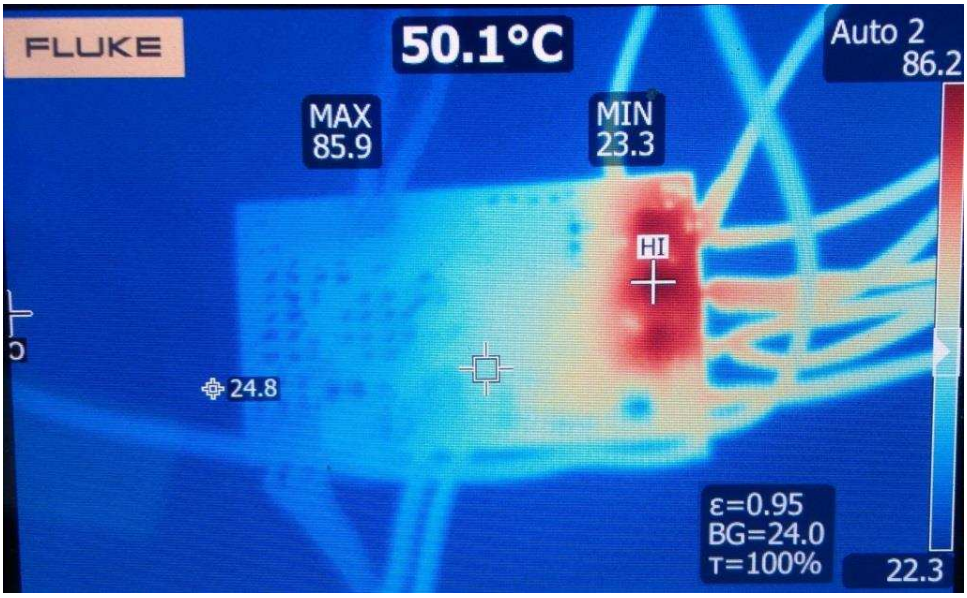

Figure 25. Thermal Image of Board With Sinusoidal Control at 2.37-A_{RMS} Winding Current

3.2.2.6 Power Stage Efficiency Test

The reference design board power stage efficiency is experimentally tested with a test setup as shown in Figure 11. Table 6 lists the test results without heat sink at a 100% duty cycle. Table 7 lists the test results without heat sink at a 95% duty cycle.

Table 6. Inverter Efficiency Test Results at 100% Duty Cycle Without Heat Sink and Without Airflow

INPUT DC VOLTAGE (V)	INPUT DC CURRENT (A)	INPUT DC POWER (W)	MOTOR WINDING RMS CURRENT (A)	BOARD OUTPUT POWER (W)	EFFICIENCY (%)
10.63	0.859	9.13	0.792	8.93	97.73
10.81	1.031	11.15	0.932	10.89	97.66
10.78	1.207	13.02	1.074	12.70	97.56
10.75	1.411	15.17	1.239	14.78	97.44
10.91	1.678	18.31	1.460	17.79	97.13
10.87	1.965	21.35	1.698	20.65	96.73
10.80	2.378	25.67	2.039	24.70	96.21
10.73	2.785	29.87	2.362	28.62	95.80
10.69	2.989	31.95	2.507	30.51	95.51

Table 7. Inverter Efficiency Test Results at 95% Duty Cycle Without Heat Sink and Without Airflow

INPUT DC VOLTAGE (V)	INPUT DC CURRENT (A)	INPUT DC POWER (W)	MOTOR WINDING RMS CURRENT (A)	BOARD OUTPUT POWER (W)	EFFICIENCY (%)
10.91	0.667	7.27	0.661	7.02	96.47
10.87	0.886	9.63	0.845	9.28	96.41
10.83	1.156	12.52	1.070	12.03	96.13
10.78	1.448	15.61	1.325	14.96	95.85
10.90	1.813	19.76	1.634	18.85	95.36
10.81	2.191	23.69	1.959	22.48	94.88
10.77	2.490	26.81	2.215	25.35	94.53
10.69	3.002	32.10	2.657	30.21	94.12

Figure 26 shows the efficiency curve of these test conditions.

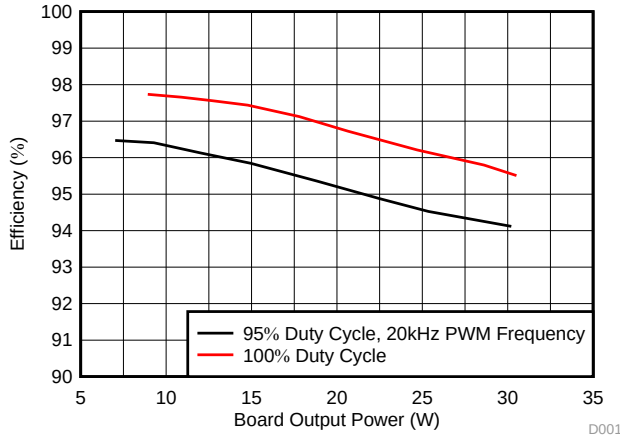

Figure 26. Power Stage Efficiency versus Output Power

The low $R_{DS(on)}$ of the CSD87502Q2 MOSFET power blocks along with clean MOSFET switching by the DRV8304 smart gate driver enable maximum three-phase inverter efficiency. The thermal pads on the MOSFET power blocks help to extract the heat to the PCB.

3.2.2.7 Overcurrent Limit Results

The gate driver DRV8304 implement adjustable V_{DS} monitors to detect overcurrent or short conditions on the external MOSFETs. The high-side V_{DS} monitors measure the voltage between the VDRAIN and SHX pins. In configuration with three current shunt amplifiers, the low-side V_{DS} monitors measure the voltage between the SHX and SPX pins.

When the voltage monitored is greater than the V_{DS} trip point ($V_{DS,OCP}$) after the V_{DS} deglitch time ($t_{DS,OCP}$) has expired, the DRV8304 detects an OCP condition and takes action according to the fault setting. In the hardware version of the DRV8304, the V_{DS} monitor acts in automatic retry mode with a 4-ms retry time.

Figure 27 shows the V_{DS} overcurrent action with the V_{DS} reference voltage set to 0.15 V.

Assuming the junction temperature of 75°C, the $R_{DS(on)}$ at 75°C ≈ 34 mΩ (approximately 1.26 times the $R_{DS(on)}$ at 25°C, from the CSD87502Q2 data sheet).

where:

- V_{DS} deglitch time ($t_{DS,OCP}$) = 4.5 µs
- Current limit threshold = V_{DS} threshold / $R_{DS(on)}$ = 4.41 A

Figure 27 shows that the current is limited at 4.6 A. Figure 28 shows the zoomed view where the PWM shuts off when the current hits the over current threshold and the fault is created. The fault resets after 4 ms.

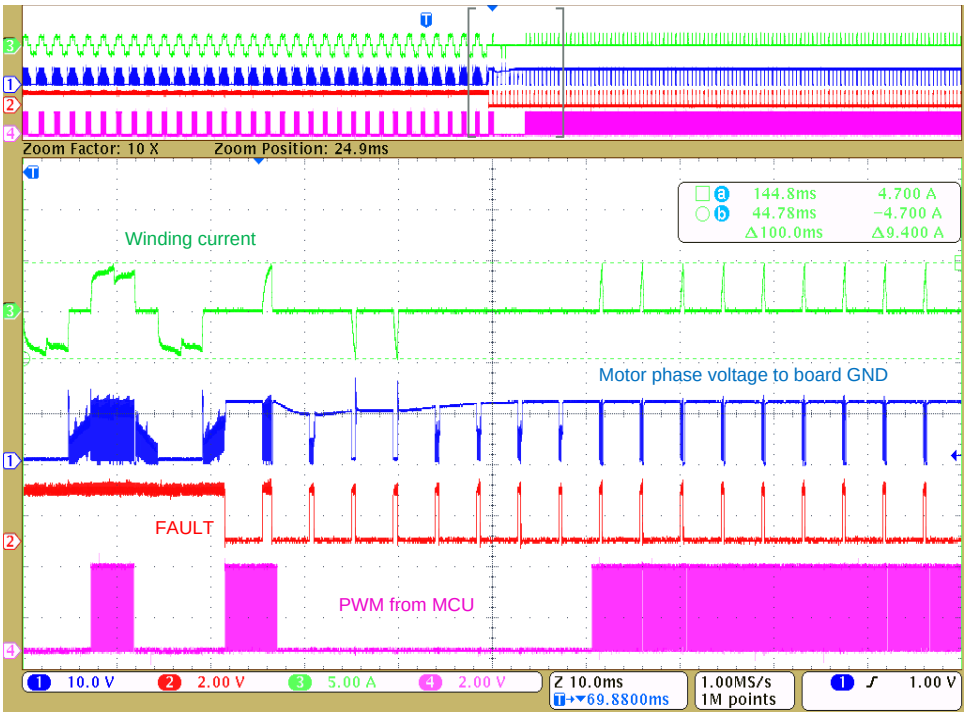

Figure 27. Overcurrent Protection With MOSFET V_{DS} Monitoring

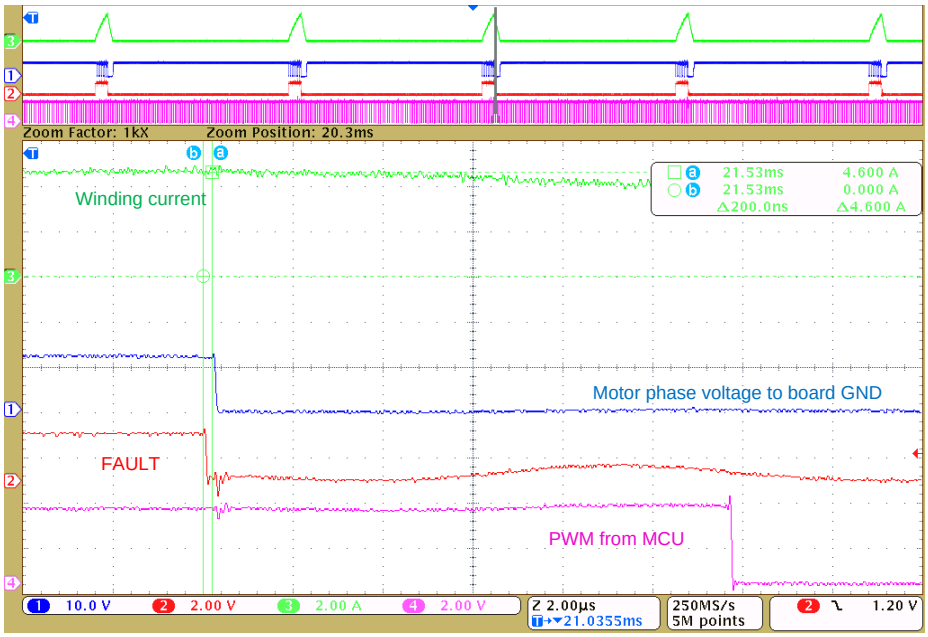

Figure 28. Zoomed View of Overcurrent Protection With MOSFET V_{DS} Monitoring

3.2.2.8 BLDC Motor 60° Electrical Position Control With Trapezoidal Excitation

Position control algorithm on the MSP430FR5949 is implemented using port interrupts capability of the MSP430 MCU. The testing is done on the BLDC motor that has three digital Hall position sensors.

Figure 29 and Figure 30 show the position control test results with a BLDC motor having four pole pairs and no gear assembly. Figure 29 shows the position control at 105° mechanical (420° electrical) with a holding torque equivalent to 2 A.

Figure 30 shows the test result with step change in mechanical position reference from 37.5° mechanical to 82.5° mechanical with a 1.5-A holding current.

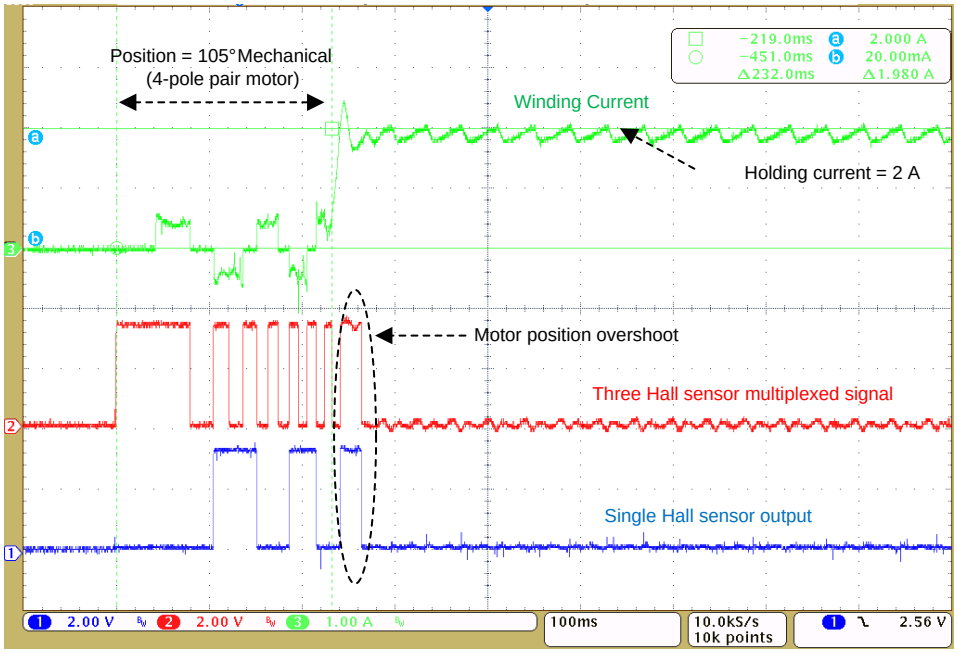

Figure 29. Test Results for Position Control at 105° Mechanical

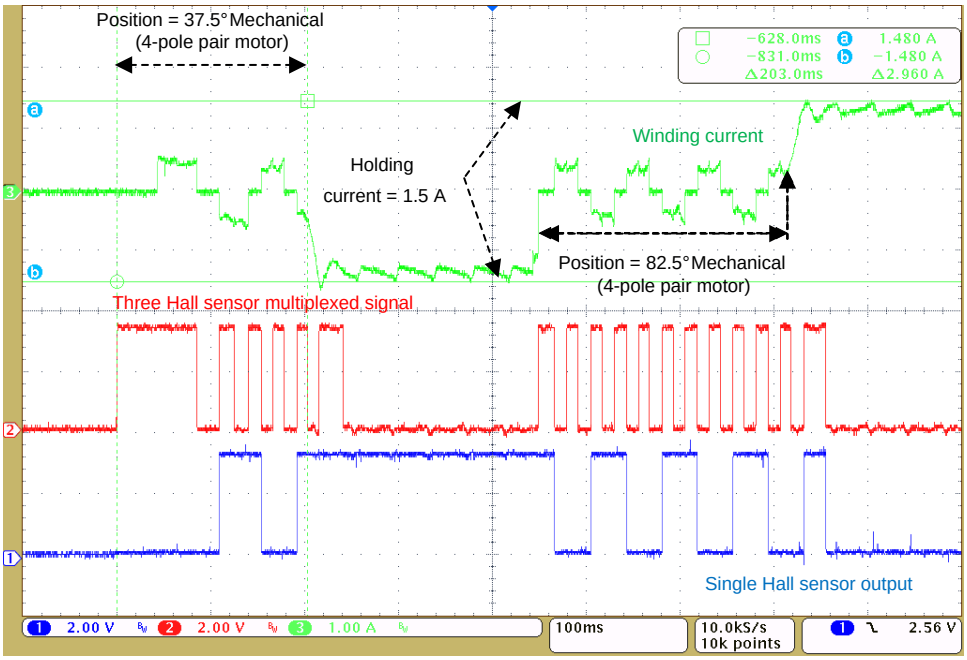

Figure 30. Test Results for Position Control With a Step Change in Position Reference

4 Design Files

4.1 Schematics

To download the schematics, see the design files at TIDA-01587.

4.2 Bill of Materials

To download the bill of materials (BOM), see the design files at TIDA-01587.

4.3 PCB Layout Recommendations

4.3.1 Layout Prints

To download the layer plots, see the design files at TIDA-01587.

4.4 Altium Project

To download the Altium project files, see the design files at TIDA-01587.

4.5 Gerber Files

To download the Gerber files, see the design files at TIDA-01587.

4.6 Assembly Drawings

To download the assembly drawings, see the design files at TIDA-01587.

5 Software Files

To download the software files, see the design files at TIDA-01587.

6 Related Documentation

1. Texas Instruments, *Field Oriented Control (FOC) Made Easy for Brushless DC (BLDC) Motors Using TI Smart Gate Drivers Application Brief*
2. Texas Instruments, *DRV8304 38-V 3-Phase Smart Gate Driver Data Sheet*

6.1 Trademarks

E2E, MSP430, Code Composer Studio are trademarks of Texas Instruments.
All other trademarks are the property of their respective owners.

7 Terminology

BLDC— Brushless DC

ESD— Electrostatic discharge

MCU— Microcontroller unit

PWM— Pulse width modulation

8 About the Authors

MANU BALAKRISHNAN is a systems engineer at Texas Instruments, where he is responsible for developing subsystem design solutions for the Industrial Motor Drive systems. Manu brings to this role his experience in power electronics and analog and mixed signal designs. He has system level product design experience in permanent magnet motor drives. Manu earned his bachelor of technology in electrical and electronics engineering from the University of Kerala and his master of technology in power electronics from National Institute of Technology Calicut, India.

VARAD JOSHI is a project trainee in the Industrial Systems team at Texas Instruments, where he is learning and developing reference design solutions with a focus on motor drive systems. Varad is a final-year student pursuing a bachelor of engineering (B.E. hons) in electrical and electronics engineering from Birla Institute of Technology & Sciences (BITS), Pilani, Goa.

JASRAJ DALVI is an end equipment lead with Industrial Systems team at Texas Instruments, where he is responsible for defining reference design solutions and control algorithms for motor control systems. He completed his bachelors of engineering degree in electrical engineering from University of Pune, India and his post-graduate diploma in marketing management at S.I.B.M. in Pune, India.

IMPORTANT NOTICE FOR TI DESIGN INFORMATION AND RESOURCES

Texas Instruments Incorporated ('TI") technical, application or other design advice, services or information, including, but not limited to, reference designs and materials relating to evaluation modules, (collectively, "TI Resources") are intended to assist designers who are developing applications that incorporate TI products; by downloading, accessing or using any particular TI Resource in any way, you (individually or, if you are acting on behalf of a company, your company) agree to use it solely for this purpose and subject to the terms of this Notice.

TI's provision of TI Resources does not expand or otherwise alter TI's applicable published warranties or warranty disclaimers for TI products, and no additional obligations or liabilities arise from TI providing such TI Resources. TI reserves the right to make corrections, enhancements, improvements and other changes to its TI Resources.

You understand and agree that you remain responsible for using your independent analysis, evaluation and judgment in designing your applications and that you have full and exclusive responsibility to assure the safety of your applications and compliance of your applications (and of all TI products used in or for your applications) with all applicable regulations, laws and other applicable requirements. You represent that, with respect to your applications, you have all the necessary expertise to create and implement safeguards that (1) anticipate dangerous consequences of failures, (2) monitor failures and their consequences, and (3) lessen the likelihood of failures that might cause harm and take appropriate actions. You agree that prior to using or distributing any applications that include TI products, you will thoroughly test such applications and the functionality of such TI products as used in such applications. TI has not conducted any testing other than that specifically described in the published documentation for a particular TI Resource.

You are authorized to use, copy and modify any individual TI Resource only in connection with the development of applications that include the TI product(s) identified in such TI Resource. NO OTHER LICENSE, EXPRESS OR IMPLIED, BY ESTOPPEL OR OTHERWISE TO ANY OTHER TI INTELLECTUAL PROPERTY RIGHT, AND NO LICENSE TO ANY TECHNOLOGY OR INTELLECTUAL PROPERTY RIGHT OF TI OR ANY THIRD PARTY IS GRANTED HEREIN, including but not limited to any patent right, copyright, mask work right, or other intellectual property right relating to any combination, machine, or process in which TI products or services are used. Information regarding or referencing third-party products or services does not constitute a license to use such products or services, or a warranty or endorsement thereof. Use of TI Resources may require a license from a third party under the patents or other intellectual property of the third party, or a license from TI under the patents or other intellectual property of TI.

TI RESOURCES ARE PROVIDED "AS IS" AND WITH ALL FAULTS. TI DISCLAIMS ALL OTHER WARRANTIES OR REPRESENTATIONS, EXPRESS OR IMPLIED, REGARDING TI RESOURCES OR USE THEREOF, INCLUDING BUT NOT LIMITED TO ACCURACY OR COMPLETENESS, TITLE, ANY EPIDEMIC FAILURE WARRANTY AND ANY IMPLIED WARRANTIES OF MERCHANTABILITY, FITNESS FOR A PARTICULAR PURPOSE, AND NON-INFRINGEMENT OF ANY THIRD PARTY INTELLECTUAL PROPERTY RIGHTS.

TI SHALL NOT BE LIABLE FOR AND SHALL NOT DEFEND OR INDEMNIFY YOU AGAINST ANY CLAIM, INCLUDING BUT NOT LIMITED TO ANY INFRINGEMENT CLAIM THAT RELATES TO OR IS BASED ON ANY COMBINATION OF PRODUCTS EVEN IF DESCRIBED IN TI RESOURCES OR OTHERWISE. IN NO EVENT SHALL TI BE LIABLE FOR ANY ACTUAL, DIRECT, SPECIAL, COLLATERAL, INDIRECT, PUNITIVE, INCIDENTAL, CONSEQUENTIAL OR EXEMPLARY DAMAGES IN CONNECTION WITH OR ARISING OUT OF TI RESOURCES OR USE THEREOF, AND REGARDLESS OF WHETHER TI HAS BEEN ADVISED OF THE POSSIBILITY OF SUCH DAMAGES.

You agree to fully indemnify TI and its representatives against any damages, costs, losses, and/or liabilities arising out of your non-compliance with the terms and provisions of this Notice.

This Notice applies to TI Resources. Additional terms apply to the use and purchase of certain types of materials, TI products and services. These include; without limitation, TI's standard terms for semiconductor products http://www.ti.com/sc/docs/stdterms.htm), evaluation modules, and samples (http://www.ti.com/sc/docs/sampterms.htm).

Mailing Address: Texas Instruments, Post Office Box 655303, Dallas, Texas 75265